



Semnan University



## Rapid mixing of Newtonian and non-Newtonian fluids in a three-dimensional micro-mixer using non-uniform magnetic field

Azam Usefian, Morteza Bayareh\*, Afshin Ahmadi Nadooshan

Department of Mechanical Engineering, Shahrekord University, Shahrekord, Iran

---

### PAPER INFO

**Paper history:**

Received: 2018-08-14

Received: 2018-12-10

Accepted: 2018-12-12

**Keywords:**

Micro-mixer;  
Magnetic field;  
Mixing efficiency;  
Electric current;  
Ferrofluid;  
Non-Newtonian fluid.

---

### ABSTRACT

The mixing of Newtonian and non-Newtonian fluids in a magnetic micro-mixer was studied numerically using  $Fe_3O_4$  ferrofluid. The mixing process was performed in a three-dimensional steady-state micro-mixer. A magnetic source was mounted at the entrance of the micro-channel to oscillate the magnetic particles. The effects of electric current, inlet velocity, size of magnetic particles, and non-Newtonian fluid were examined on the mixing efficiency. It was demonstrated that the mixing efficiency would increase with applied current and the size of magnetic particles. The inlet velocity has an inverse effect on the enhancement of the mixing efficiency. It is found that electric currents of 0A and 50A would lead to the mixing efficiency of 10% and 83%, respectively. In addition, the results of the present work revealed that the mixing efficiency of a non-Newtonian fluid (blood) is smaller than that of a Newtonian one.

DOI: 10.22075/jhmtr.2018.15611.1218

---

© 2019 Published by Semnan University Press. All rights reserved.

### 1. Introduction

Micro-mixer is one of the most important components of microfluidic or lab-on-a-chip devices. Biochemical processes, DNA analysis, and micro-reactors are some applications of these systems in which the rapid mixing of fluids is essential. Since the flow regime in microfluidic devices is laminar ( $Re < 1$ ), the mixing process happens due to the diffusion at the interface of the fluids. Hence, a homogeneous mixing would be obtained in a very long period of time due to a very small diffusion coefficient of microfluidic solutions in the order of  $10^{-10} m^2/s$  [1].

Micro-mixers are generally categorized into active and passive mixers. In active micro-mixers, an external moving part disturbs the fluids. However, passive mixers have no external excitation part. The mixing efficiency of active mixers is much higher than that of passive ones due to the incorporation of an external excitation source in the

flow. In passive mixers, the mixing efficiency directly depends on the special design of the macro-channel.

Numerous designs have been presented for active micro-mixers. These schemes utilize electrical field [2-4], magnetic field [5-7], pressure field [8-10], or sound field [11-13]. Active micro-mixers would utilize Magneto-Hydro-Dynamics (MHD) to improve the stirring efficiency. These mixers use AC or DC electric and magnetic fields so as to agitate fluids using Lorentz force [14]. It should be mentioned that MHD is utilized only for conductive fluids. Most of the micro-scale biological systems contain fluids that are not conductive. Hence, the suspension of magnetic particle and biological solutions allows us to use MHD and enhance mixing [15].

Wang et al. [1] studied the effect of magnetic force and operating frequency on the mixing efficiency in a micro-channel. They found that the optimum operating frequency is a function of microchannel width. The optimal frequency leads to a mixing efficiency of 97.7% in a period

---

\*Corresponding Author: M. Bayareh, Department of Mechanical Engineering, Shahrekord University, Shahrekord, Iran.  
Email: m\_bayareh@yahoo.com.

of time  $t = 1.1$  s at  $x = 500 \mu\text{m}$  and the volume fraction of 5.7%. Nouri et al. [7] investigated the mixing process in a Y-shaped magnetic micro-mixer experimentally and numerically. They used a permanent magnet and found that 2000 G magnet can enhance 90% the mixing efficiency. Their results demonstrated that as the Ferrofluid flow rate increases, the mixing efficiency decreases and equivalently, the mixing length increases. Tsai et al. [16] evaluated the mixing process in a Y-shaped micro-mixer contains Ferro-nanofluid and water using a permanent magnetic field. They concluded that the permanent magnet leads to the mixing efficiency of 90%, while it is below 15% in the absence of the magnetic field. The influence of the arrangement of magnetic particles on mixing efficiency of a micro-mixer was studied by Kamali et al. [17]. They showed that the random distribution of magnetic particles leads to lower mixing efficiency in comparison with their determined position. Kefou et al. [18] studied the mixing phenomenon in an MHD macro-mixer to purify water from metals. They utilized two electromagnets to apply a homogeneous magnetic field and revealed that oscillating magneto nanoparticles enhance the mixing efficiency. Ergin et al. [19] investigated the transient flow field in a magnetic micro-mixer. The main objective of their work was to measure the velocity and estimate the interface location experimentally. Kitenebergs et al. [20] performed experimental investigations to enhance mixing efficiency in microfluidic systems. They reported that the mixing efficiency would be enhanced four times in a microfluidic device that employs magnetic particles in comparison with a simple device in which the mixing happens due to diffusion mechanism. They also concluded that the mixing with magnetic particles is 10 times faster than that with diffusion. The comparison between recent trends for active micro-mixers was presented by Cai et al. [21]. Recently, Meister et al. [22] investigated the effect of pumped recirculation on the mixing of Newtonian and pseudo-plastic non-Newtonian fluids in anaerobic digesters by different impellers. They demonstrated that the highest mixing quality would be obtained using the proposed model. They optimized the value of impeller angular velocity for a total solids concentration. The combined effect of pulsatile flow and electro-osmosis on mixing characteristics of Newtonian and non-Newtonian fluids was studied by Tatlisoz and Canpolat [23]. They concluded that rectangular obstacles for non-Newtonian fluids are required to obtain the same mixing efficiency for Newtonian fluids under similar conditions.

To the best of our knowledge, there has been no study performed on the effects of non-uniform magnetic source on the mixing efficiency in a three-dimensional micro-mixer. The main objective of the present work is to explore the influence of non-uniform magnetic field on the mixing efficiency in a micro-mixer. In addition, the present numerical simulations are performed in three dimensions, and the non-Newtonian fluids were considered using Carreau-Yasuda's model so as to study the effect of

magnetic field on these fluids like blood. The influence of current intensity and inlet fluid velocity on mixing efficiency was studied. The paper is organized as follows: the governing equations are presented in Section 2. In Section 3, the numerical method is described, and the results are discussed in Section 4. Conclusions are presented in Section 5.

## 2. Governing equations

The governing equations for a three-dimensional incompressible flow are continuity and momentum equations:

$$\nabla \cdot \vec{V} = 0 \quad (1)$$

$$\rho_f \left( \frac{\partial \vec{V}}{\partial t} + \vec{V} \cdot \nabla \vec{V} \right) = -\nabla P + \nabla \cdot \vec{\tau} + \vec{F}_m \quad (2)$$

Where,  $\vec{V}$  indicates the velocity vector,  $P$  is the pressure,  $\rho_f$  is the fluid density and  $\mu$  is the dynamic viscosity.  $\vec{\tau} = \mu \vec{\gamma}$  denotes the shear stress tensor and  $\vec{F}_m$  refers to the magnetic force. The dynamic viscosity has a constant value for Newtonian fluids. Since most of the biological fluids are non-Newtonian, and they are considered in the present study as a part of the simulations, dynamic viscosity for these fluids is presented based on Carreau-Yasuda's model:

$$\mu = \mu_\infty + (\mu_0 - \mu_\infty) [1 + (\lambda \vec{\gamma})^2]^{\frac{n-1}{2}} \quad (3)$$

where  $\mu_0$  is the zero shear rate viscosity,  $\mu_\infty$  is an infinite shear rate viscosity, and  $\lambda$  is a time constant. Constant  $n$  is the power-law index that accounts for the shear thinning behavior of the model. The strain rate tensor  $\vec{\gamma}$  is defined as:

$$\vec{\gamma} = (\nabla \vec{V}) + (\nabla \vec{V})^T \quad (4)$$

The magnetic force  $\vec{F}_m$  is due to the magnetic field that is exerted to the particles [24]:

$$\vec{F}_m = \mu_0 (\vec{M} \cdot \nabla) \vec{H} \quad (5)$$

$\mu_0 (\vec{M} \cdot \nabla) \vec{H}$  is the Kelvin force density due to the electromagnetic field.  $\vec{M}$  is the magnetization, which is expressed as [24]:

$$\vec{M} = M_s L(\xi) = \frac{6\alpha_p m_p}{\pi d_p^3} (\coth(\xi) - \frac{1}{\xi}) \quad (6)$$

The particle magnetic moment  $m_p$  is defined as [24]:

$$m_p = \frac{4\mu_B \pi d_p^3}{6 \times 91.25 \times 10^{-30}} \quad (7)$$

and  $\xi$  is the Langevin parameter as follows [24]:

$$\xi = \frac{\mu_0 m_p \alpha_p}{k_B T} \quad (8)$$

In addition,  $\vec{H}$  is the magnetic field strength defined according to Biot-Savart law [25]:

$$H(x, y) = \frac{I}{2\pi} \frac{1}{\sqrt{(x-a)^2 + (y-b)^2}} \quad (9)$$

The schematic of the present problem and the electromagnetic force at the macro-channel is shown in Fig. 1. The magnetic source is located at (a, b). Applied current is in the z-direction. The magnetic field is strong at the source point and decreases with increasing the distance from the source.  $Fe_3O_4$  nanoparticles are utilized to disturb the fluid flow. The volume fraction of

nanoparticles is  $\varphi = 5\%$ . The properties of  $Fe_3O_4$  nanoparticles are presented in Table 1. The transport-diffusion equation of streams A and B is expressed as:

$$\vec{V} \cdot \nabla C = D \Delta^2 C \quad (10)$$

where C and D indicate the concentration and the diffusion coefficient of the ferrofluid, respectively.

The density and viscosity of the mixture are described as following [7]:

$$\rho_m = C \rho_{ferro} + (1 - C) \rho_w \quad (11)$$

$$\mu_m = \mu_{ferro} EXP[(C - 1) \ln(1 + 2.5C)] \quad (12)$$

where subscripts m, ferro, and w correspond to the mixture, the ferrofluid, and water, respectively.

Mixing efficiency, ME, is calculated in order to quantify the performance of the micro-mixer:

$$ME = 1 - \frac{\left[ \sum_{i=1}^N \frac{(c_i - \bar{c})^2}{N} \right]^{1/2}}{\bar{c}} \approx 1 - \frac{\sigma_c}{\bar{c}} \quad (13)$$

where  $\sigma_c$  and  $\bar{c} = \sum_{i=1}^N c_i / N$  are the standard deviation and the average concentration, respectively. N denotes the number of nodes in the considered area ( $N = 15$ ). Therefore,  $ME = 100\%$  indicates a perfect mixing.

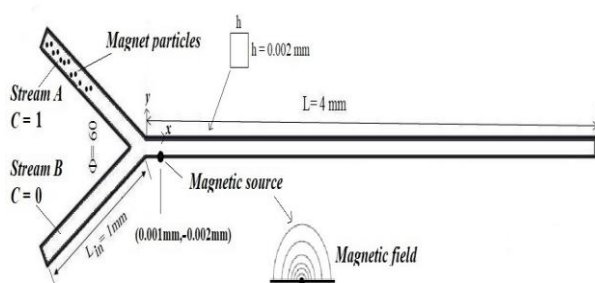


**Figure 1.** Schematic of a magnetic micro-mixer.

**Table 1.** Properties of  $Fe_3O_4$  nanoparticles.

Property	value
$\rho_p$	5200 ( $kg/m^3$ )
$m_p$	$2.27 \times 10^{-21}$ ( $kg$ )
$r_p$	$5 \times 10^{-9}$ ( $m$ )

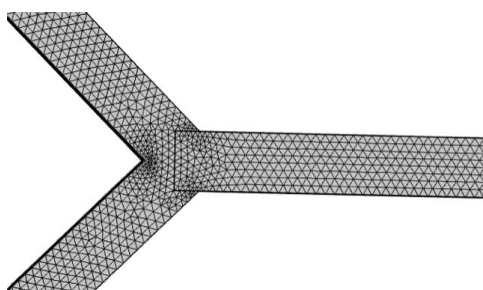


**Figure 2.** Geometrical discretization of the micro-mixer.

### 3. Numerical method

The governing equations for laminar incompressible flow were solved using a finite-element method. The commercial software COMSOL Multiphysics 5.2a was employed to solve the mathematical models. The Navier-Stokes equations include the magnetic force  $\vec{F}_m$ . The magnetization, the particle magnetic moment, and the Langevin parameter were defined so as to calculate the magnetic force. The computational domain was discretized by unstructured triangular meshes. The grid resolution was performed using pre-defined fine element size to extra fine element size, and pre-defined extra fine element size was used for the computational domain. Part of the grid profile of the considered geometry is shown in Fig. 2. Size parameters for the grid elements are as follow: the number of elements is 135513, minimum element quality is 0.1057, and average element quality is 0.6273. The present simulations indicate that further mesh refinement does not affect the magnitude of the mixing index. No-slip boundary condition was imposed on all walls. The pressure outlet boundary condition was used for the micro-mixer exit. The ferrofluid concentration was considered as 1 and 0 for stream A and B, respectively. In addition, the outflow boundary condition was employed for transport-diffusion equation.

## 4. Results

### 4.1 Validation

In order to verify the present simulations, the numerical results were compared to the experimental results of Nouri et al. [7] who studied the influence of permanent magnetic field on the mixing efficiency of a Y-shaped micro-mixer (Fig. 3). The figure demonstrates the mixing efficiency along the micro-channel and shows that the present results are in a very good agreement with the experimental ones. It should be mentioned that the experimental results correspond to the steady-state condition ( $t = 80s$ ).

### 4.2 Effect of inlet velocity

In order to evaluate the effect of flow rate (inlet velocity) on the mixing efficiency, different Reynolds numbers were considered. The Reynolds number is defined as:

$$Re = \frac{\rho_w U_{in} h}{\mu_w} \quad (14)$$

Fig. 4 shows the concentration contours of the magnetic micro-mixer for different Reynolds numbers for  $I = 50$  mA,  $n = 1$ , and  $\varphi = 0.05$ . The concentration of ferrofluid and water are represented by red and blue colors, respectively. Green color represents completed concentration. The figure shows that as the inlet velocity (Reynolds number) increases, the mixing quality decreases.

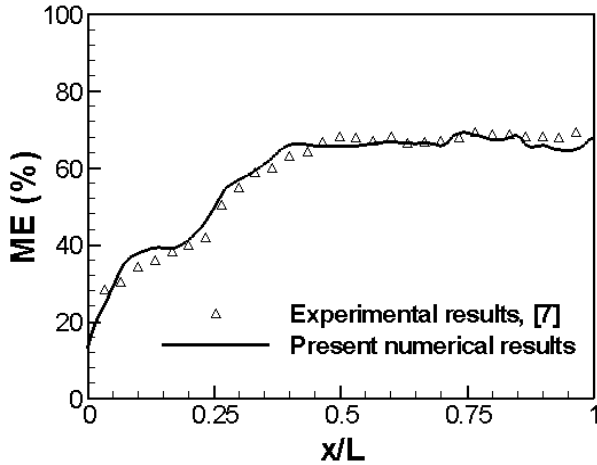


**Figure 3.** Mixing efficiency along the micro-channel for  $\varphi = 2.5\%$  and  $H = 3000\text{G}$ .

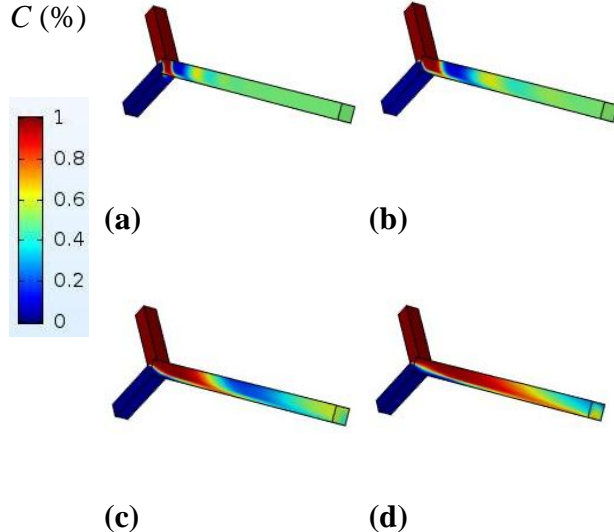


**Figure 4.** Concentration contours at different Reynolds numbers for  $I = 50\text{ A}$ ,  $n = 1$ , and  $\varphi = 0.05$ : (a)  $\text{Re} = 5$ , (b)  $\text{Re} = 10$ , (c)  $\text{Re} = 25$ , and (d)  $\text{Re} = 50$ .

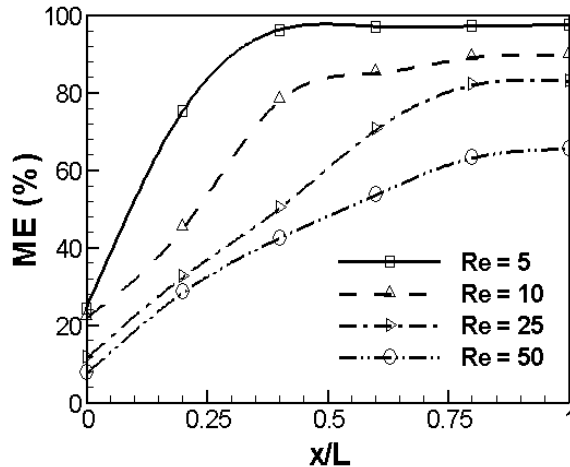


**Figure 5.** Mixing efficiency along the micro-channel at different Reynolds numbers for  $I = 50\text{ A}$ ,  $n = 1$ , and  $\varphi = 0.05$ .

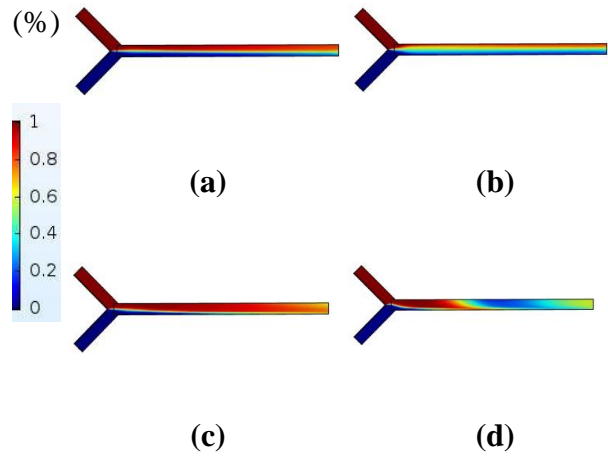


**Figure 6.** Concentration contours in the central plane at different electric currents for  $\text{Re} = 25$ ,  $n = 1$ , and  $\varphi = 0.05$ : (a)  $I = 0\text{A}$ , (b)  $I = 10\text{A}$ , (c)  $I = 25\text{A}$ , and (d)  $I = 50\text{A}$ .

In order to quantify the results, mixing efficiency along the mixing channel is plotted in Fig. 5. It was found that mixing efficiency enhances with decreasing the flow rate. This is due to the fact that at lower Reynolds numbers, the fluids have enough time to mix completely. Also, it can be concluded that the mixing length increases with the Reynolds number. Nouri et al. [7] showed that there is a linear relationship between the mixing length and the flow rate for the case of a permanent magnetic field. Fig. 5 indicates that for  $\text{Re} = 5$ , only the mixing length  $x = 0.43L$  is required to reach a complete mixture. This value for  $\text{Re} = 10$  and  $\text{Re} = 25$  is  $x = 0.78L$  and  $x = 0.94L$ , respectively. These values demonstrate that there is not a linear relationship between the flow rate and the mixing length for the present simulations.

#### 4.3 Effect of the magnetic field

In this section, the influence of magnetic force is studied by changing the applied current and size of the magnetic particles. Several parameters affect the magnetic force, including applied current, nanoparticle size, the magnetization of nanoparticles, and the position of a magnetic source. Here, two first factors are considered. Since a magnetic source is employed in the present simulations, the maximum magnetic force occurs at  $x = 100\mu\text{m}$  cross-section ( $x = 100\mu\text{m}$ ,  $0 < y < 2\mu\text{m}$ , and  $0 < z < 2\mu\text{m}$ ). The magnetic field strength is obtained using Eq. (9) for different electric currents and the magnetic force is calculated from the Eq. (5).

##### a. Electric current effect

Different values of electric current ( $I = 5, 10, 25$ , and  $50\text{ A}$ ) were considered to evaluate the influence of applied current on mixing efficiency. Concentration contours are presented in Fig. 6 for  $n = 1$ ,  $\varphi = 0.05$ ,  $\text{Re} = 25$ , and different electric currents. This figure qualitatively shows that the mixing efficiency increases with applied currents.

The concentration contours for no magnetic force is also presented in this figure. The mixing mechanism for this case is the only diffusion, and the mixing efficiency is small and remains approximately constant (see Fig. 6). This finding is consistent with the results of Wang et al. [1]. Fig. 7 shows the mixing efficiency along the channel quantitatively. At low electric currents, the amplitude of oscillation of magnetic particles in the lateral direction is small. Therefore, most of the particles do not reach the interface. In other words, a small fraction of the particles collide with the interface and disturb it. Hence, the low mixing efficiency is obtained for low applied currents. For instance, the mixing efficiency at the exit of the micro-mixer is approximately 38.9% for  $I = 5\text{ A}$ . As the oscillation of magnetic particles in the lateral direction increases, the mixing enhances. For  $I = 50\text{ A}$ , the mixing efficiency at the exit of the micro-mixer reaches 83.25%. It can be concluded that the mixing length in which a complete mixing occurs, decreases with the electric current.

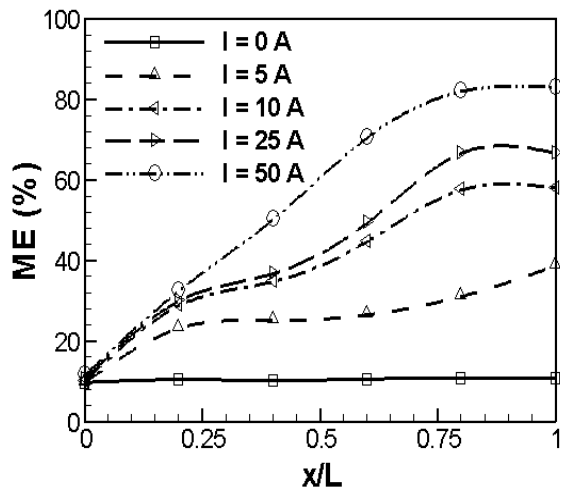


**Figure 7.** Mixing efficiency along the micro-channel for different electric currents at  $\text{Re} = 25$ ,  $n = 1$ , and  $\varphi = 0.05$ .

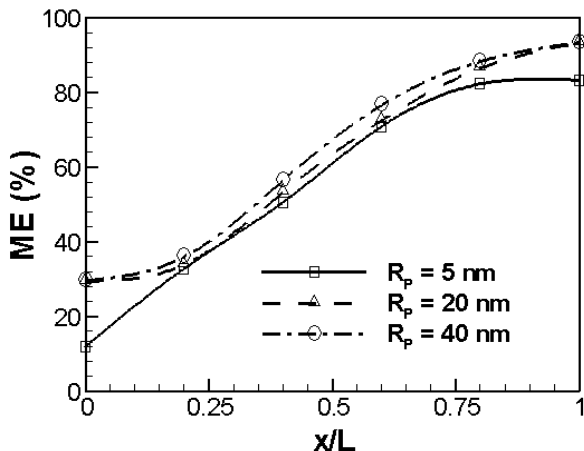


**Figure 8.** Mixing efficiency along the micro-channel for different sizes of magnet particles at  $\text{Re} = 25$ ,  $n = 1$ ,  $I = 50\text{ A}$ , and  $\varphi = 0.05$ .

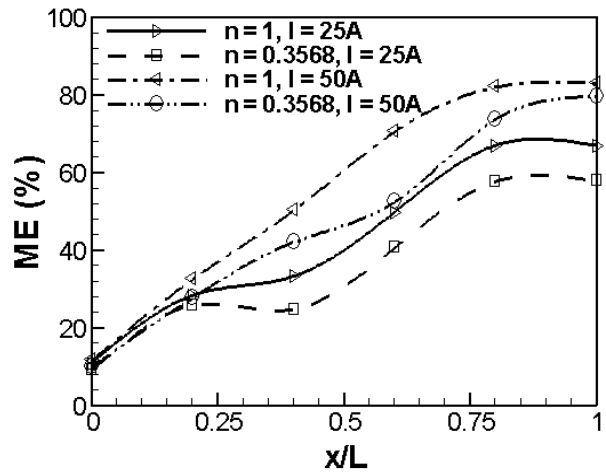


**Figure 9.** Mixing efficiency along the micro-channel for non-Newtonian fluid (blood) in comparison with Newtonian one at  $\text{Re} = 25$  and  $\varphi = 0.05$ .

#### b. Particle size effect

One of the parameters affecting the magnetic force is the size of magnetic particles. Fig. 8 shows the mixing efficiency along the micro-channel for different nanoparticle radii at  $\text{Re} = 25$  and  $I = 50\text{ A}$ .

As the size of the magnetic particles increases, they exhibit two opposite effects. The disturbance of larger particles is higher than that of smaller ones. However, larger particles need a stronger magnetic force to oscillate in the lateral direction. In other words, there is a competition between these effects. Enhancement of the radius of magnetic particles from  $5\text{ nm}$  to  $40\text{ nm}$  would lead to an increase of 7.7% in the mixing efficiency at the exit of the micro-channel. The figure demonstrates that the mixing efficiency corresponds to  $R_p = 20\text{ nm}$  is approximately equal to that corresponds to  $R_p = 40\text{ nm}$ . It can be concluded that the effect of the size of magnetic particles is not considerable in comparison with the electric field.

#### 4.4 Non-Newtonian fluid

Rapid mixing is of considerable importance in a variety of biological applications, especially in lab-on-a-chip systems. Blood is a non-Newtonian fluid where its viscosity depends on the shear rate and suspension of viscoelastic particles. There are several non-Newtonian models commonly used for simulation of human blood flow: Power-law, Carreau, Carreau-Yasuda, Casson, and Walburn-Schnecke [26]. In the present work, the Carreau-Yasuda model was used to evaluate its non-Newtonian behavior during the mixing process. It should be mentioned that this model is an appropriate one for modeling the shear-thinning fluids. According to Eq. (3), three constants of the model for human blood are:  $\mu_0 = 0.056\text{ Pa.s}$ ,  $\mu_\infty = 0.0035\text{ Pa.s}$ ,  $\lambda = 3.313$ , and  $n = 0.3568$ .

It was known that the mixing quality is significantly affected by shear-dependent viscosity of shear-thinning and shear-thickening fluids [27]. Kunti et al. [27] used the power-law model for non-Newtonian fluids and demonstrated that the mixing efficiency increases as the power-law index of non-Newtonian fluids increases. They concluded that the mixing quality of the dilatant fluids ( $n>1$ ) is higher than that of Newtonian ( $n=1$ ) and pseudoplastic ( $n<1$ ) fluids. In the present work, for the case of a shear-thinning fluid (blood), it was revealed that the mixing efficiency increases with the power-law index. Fig. 9 shows that the mixing efficiency of blood decreases for two applied currents  $I = 25$  and  $50$  A in comparison with the Newtonian fluid. In addition, mixing characteristics of two-phase flows can be determined using different schemes such as front tracking methods [28-30].

## 5. Conclusions

Rapid mixing in a magnetic micro-mixer consisted of a magnetic source was studied numerically. The enhancement of mixing efficiency was evaluated in terms of a ferrofluid by COMSOL Multi-physics 5.2a computational software. The results demonstrated that the magnetic force has a significant effect on the mixing efficiency where the electric current changes. However, the effect of the size of magnetic particles is not considerable. It was shown that the mixing process improves as the inlet velocity of fluids decreases. The results also revealed that the mixing quality of Newtonian fluids is higher than that of shear-thinning one (blood) for constant magnetic force.

## Nomenclature

$a, b$	Magnetic source coordinates (m)
$C$	The concentration coefficient of the ferrofluid
$D$	The diffusion coefficient of the ferrofluid
$\vec{F}_m$	The magnetic force (N)
$h$	The macrochannel height (m)
$\vec{H}$	The magnetic field strength (N.m/A)
$m_p$	The particle magnetic moment (A)
$\vec{M}$	The magnetization (A/m)
ME	The mixing efficiency
P	The pressure (Pa)
Re	Reynolds number
t	time (s)
$\vec{V}$	The velocity vector (m/s)
x, y	The coordinates (m)

## Greek letters

$\rho$	The density (kg/m <sup>3</sup> )
$\mu$	The dynamic viscosity (Pa.s)
$\lambda$	Time constant (s)
$\vec{\gamma}$	The strain rate tensor
$\sigma_c$	The standard deviation
$\xi$	The Langevin parameter
$\varphi$	The volume fraction of nanoparticles

## References

- [1] Y. Wang, J. Zhe, T.F. Cheng, A rapid magnetic particle driven micromixer, *Microfluid and Nanofluid*, 4, 375-389, (2008).
- [2] G. R. Wang, F. Yang, W. Zhao, There can be turbulence in microfluidics at low Reynolds number. *Lab on a Chip*, 14, 1452-1458, (2014).
- [3] Y. Wu, Y. Ren, Y. Tao, L. Hou, Q. Hu, H. Jiang, A novel micro-mixer based on the alternating current-flow field effect transistor. *Lab on a Chip*, 17, 186-197, (2016).
- [4] T. Zhou, H. Wang, L. Shi, Z. Liu, S. Joo, An enhanced electro-osmotic micro-mixer with an efficient asymmetric lateral structure. *Micromachines*, 7, 218 (2016).
- [5] M. La, W. Kim, W. Yang, H.W. Kim, D.S. Kim, Design and numerical simulation of complex flow generation in a micro-channel by magneto-hydro-dynamic (MHD) actuation. *International Journal of Precision Engineering and Manufacturing*, 15, 463-470, (2014).
- [6] M. Chang, J. L. F. Gabayno, R. Ye, K.-W. Huang, Y.-J. Chang, Mixing efficiency enhancing in micro-mixer by controlled magnetic stirring of fe<sub>3</sub>o<sub>4</sub> nanomaterial. *Microsystem Technologies*, 23, 457-463, (2016).
- [7] D. Nouri, A. Zabihi-Hesari, M. Passandideh-Fard, Rapid mixing in micro-mixers using magnetic field. *Sensors and Actuators A: Physical*, 255, 79-86, (2017).
- [8] M. Du, Z. Ma, X. Ye, Z. Zhou, On-chip fast mixing by a rotary peristaltic micro-pump with a single structural layer. *Science China Technological Sciences*, 56, 1047-1054 (2013).
- [9] Y. Abbas, J. Miwa, R. Zengerle, F. von Stetten, Active continuous-flow micro-mixer using an external braille pin actuator array. *Micromachines*, 4, 80-89, (2013).
- [10] Q. Xia, S. Zhong, Liquid mixing enhanced by pulse width modulation in a y-shaped jet configuration. *Fluid Dynamics Research*, 45, 025504 (2013).
- [11] H. V. Phan, M.B. Coskun, M. Sesen, G. Pandraud, A. Neild, T. Alan, Vibrating membrane with discontinuities for rapid and efficient microfluidic mixing. *Lab on a Chip*, 15, 4206-4216, (2015).
- [12] P. H. Huang, Y. Xie, D. Ahmed, J. Rufo, N. Nama, Y. Chen, C.Y. Chan, T.J. Huang, An acoustofluidic micro-mixer based on oscillating sidewall sharp-edges. *Lab on a Chip*, 13, 3847-3852, (2013).
- [13] S. Orbay, A. Ozcelik, J. Lata, M. Kaynak, M. Wu, T. J. Huang, Mixing high-viscosity fluids via acoustically driven bubbles. *Journal of*

- Micromechanics and Microengineering, 27, 015008, (2017).
- [14] J. West, B. Karamata, B. Lillis, Application of magneto-hydro-dynamic actuation to continuous flow chemistry. *Lab on a Chip*, 2, 224–230, (2002).
- [15] H. Suzuki, C.M. Ho, N. Kasagi, A chaotic mixer for magnetic bead-based micro cell sorter. *Journal of Microelectromechanical Systems*, 13, 779–790, (2004).
- [16] T. H. Tsai, D.S. Liou, L.S. Kuo, P.H. Chen, Rapid mixing between ferro-nanofluid and water in a semi-active Y-type micromixer, *Sensors and Actuators A: Physical*, 153, 267–273, (2009).
- [17] R. Kamali, S.A. Shekoohi, A. Binesh, Effects of magnetic particles entrance Arrangements on mixing efficiency of a magnetic bead micromixer, *Nano-Micro Letter*, 6(1), 30-37, (2014).
- [18] N. Kefou, E. Karvelas, K. Karamanos, T. Karakasidis, I.E. Sarris, Water purification in micromagnetofluidic devices: mixing in MHD micromixers, *Procedia Engineering*. 162, 593-600, (2016).
- [19] F. G. Ergin, B.B. Watz, K. Erglis, A. Cebers, Time-resolved velocity measurements in a magnetic micromixer, *Experimental Thermal and Fluid Science*, 67, 6-13, (2015).
- [20] G. Kitenebergs, K. Erglis, R. Perzynski, A. Cebers, Magnetic particle mixing with magnetic micro-convection for microfluidics, *Journal of Magnetism and Magnetic Materials*, 380, 227-230, (2015).
- [21] G. Cai, L. Xue, H. Zhang, J. Lin, A review on micromixers, *Micromechanics*, 8, 1-27, (2017).
- [22] M. Meister, M. Rezavand, C. Ebner, T. Pumpel, W. Rauch, Mixing non-Newtonian flows in anaerobic digesters by impellers and pumped recirculation, *Advances in Engineering Software*, 115, 194-203, (2018).
- [23] M. M. Tatlisoz, C. Canpolat, Pulsatile flow micromixing coupled with ICEO for non-Newtonian fluids, *Chemical Engineering and Processing: Process Intensification*, 131, 12-19, (2018).
- [24] H. Yamaguchi, *Engineering Fluid Mechanics*, Netherlands: Springer Science, (2008).
- [25] E. E. Tzirtzilakis, N.G. Kafoussias, Three-Dimensional Magnetic Fluid Boundary Layer Flow over a Linearly Stretching Sheet, *Journal of Heat Transfer*, 132, 11701–11708, (2010).
- [26] M. Cavazzuti, M. Atherton, M. W. Collins, G. S. Barozzi, Non-Newtonian and flow pulsatility effects in simulation models of a stented intracranial aneurysm, *Journal of Engineering in Medicine*, 225, 597-609, (2011).
- [27] G. Kunti, A. Bhattacharya, S. Chakraborty, Analysis of micromixing of non-Newtonian fluids driven by alternating current electrothermal flow, *Journal of Non-Newtonian Fluids*, 247, 123-131, (2017).
- [28] M. Bayareh, S. Mortazavi, Effect of density ratio on the hydrodynamic interaction between two drops in simple shear flow, *Iranian Journal of Science and Technology*, 35, 441-452, (2011).
- [29] M. Bayareh, S. Mortazavi, Migration of a drop in simple shear flow at finite Reynolds numbers: size and viscosity ratio effects, *Proceeding of International Conference on Mechanical, Industriel and Manufacturing Engineering (ICMIME)*, Cape Town, South Africa, (2010).
- [30] M. Bayareh, S. Mortazavi, Geometry effects on the interaction of two equal-sized drops in simple shear flow at finite Reynolds numbers, *5th International Conference: Computational Methods in Multiphase Flow*, WIT Trans. Eng. Sci., 63, 379-388, (2009).